

REGULARISED INTEGRAL EQUATIONS FOR CRACK SHAPE  
DETERMINATION PROBLEMS

Naoshi Nishimura (西村 直志)

Department of Civil Engineering, Kyoto University

1. Introduction

Let  $D$  be a bounded domain in  $R^2$  having a smooth boundary  $\partial D$ . This domain  $D$  contains a smooth piece of non-self-intersecting curve  $S$ , or a *crack*, in its interior. The shape and the location of  $S$ , however, remain unknown. We are now interested in determining such geometrical information of  $S$  from experimental data obtained in boundary measurements. To be specific we consider a measurement using a physical quantity  $u$  governed by Helmholtz' equation

$$(\Delta + k^2)u = 0 \quad \text{in } D \setminus \bar{S}, \quad (1.1)$$

where  $k \geq 0$  is the wave number. This quantity  $u$  is assumed to satisfy

$$\left(\frac{\partial u(\mathbf{x})}{\partial n}\right)^\pm = 0 \quad \text{on } S, \quad \lim_{x(\in S) \rightarrow x_0(\in \partial S)} \varphi(\mathbf{x}) = 0, \quad (1.2), (1.3)$$

where  $\varphi(\mathbf{x}) := u^+(\mathbf{x}) - u^-(\mathbf{x})$  and the superposed  $+$  ( $-$ ) indicates the limit from the positive (negative) side, with the positive side of  $S$  indicating the one into which the unit normal vector  $\mathbf{n}$  to  $S$  points. We now carry out measurements which can be interpreted as prescribing Dirichlet data on  $\partial D$  and measuring the corresponding Neumann data, or vice versa. As a result of these boundary measurements, we know several pairs of both Dirichlet and Neumann data on  $\partial D$  denoted by  $\overset{\circ}{u}^I$  and  $\partial \overset{\circ}{u}^I / \partial n$  for  $I = 1 \sim M$ , where  $M$  is the number of experiments. From these data we attempt to reconstruct  $S$ .

Problems of this type in the Laplace case ( $k = 0$ ) have been considered by engineers as well as by mathematicians; some of these efforts are found in references cited in [1] and in [2]. Also we point out that this problem is related to another of determining the shape of an ordinary (non-flat) scatterer from far field patterns considered in [3], [4], etc. In this paper we shall discuss a numerical method of solving our inverse problem with the help of the so called boundary integral equation method (BIEM).

## 2. Direct and inverse problems

To begin with, we discuss the direct problem, where the shape and the location of  $S$  are known. Our problem is to solve (1.1) subject to (1.2), (1.3) and a boundary condition of either Dirichlet or Neumann type on  $\partial D$ . The solution to this problem is known to have the following integral representation:

$$u(\mathbf{x}) = \int_{\partial D} G(\mathbf{x} - \mathbf{y}) \frac{\partial u(\mathbf{y})}{\partial n} ds_y - \int_{\partial D} \frac{\partial G(\mathbf{x} - \mathbf{y})}{\partial n_y} u(\mathbf{y}) ds_y + \int_S \frac{\partial G(\mathbf{x} - \mathbf{y})}{\partial n_y} \varphi(\mathbf{y}) ds_y, \quad (2.1)$$

where  $G(\mathbf{x} - \mathbf{y})$  is the fundamental solution of Helmholtz' equation given by

$$G(\mathbf{x} - \mathbf{y}) = \frac{i}{4} H_0^{(1)}(k|\mathbf{x} - \mathbf{y}|), \quad k \neq 0$$

and  $H_0^{(1)}$  is the Hankel function of the first kind and 0th order. The unknown data on  $\partial D$  (either  $u$  or  $\partial u/\partial n$ ) and  $\varphi$  on  $S$  are obtained as the solution to the following system of 'integral' equations:

$$0 = \frac{u(\mathbf{x})}{2} - \int_{\partial D} G(\mathbf{x} - \mathbf{y}) \frac{\partial u(\mathbf{y})}{\partial n} ds_y + \int_{\partial D} \frac{\partial G(\mathbf{x} - \mathbf{y})}{\partial n_y} u(\mathbf{y}) ds_y - \int_S \frac{\partial G(\mathbf{x} - \mathbf{y})}{\partial n_y} \varphi(\mathbf{y}) ds_y, \quad \mathbf{x} \in \partial D \quad (2.2)$$

$$0 = \frac{\partial}{\partial n_x} \left( \int_{\partial D} G(\mathbf{x} - \mathbf{y}) \frac{\partial u(\mathbf{y})}{\partial n} ds_y - \int_{\partial D} \frac{\partial G(\mathbf{x} - \mathbf{y})}{\partial n_y} u(\mathbf{y}) ds_y \right) + \int_S \frac{\partial}{\partial n_x} \frac{\partial}{\partial n_y} G(\mathbf{x} - \mathbf{y}) \varphi(\mathbf{y}) ds_y, \quad \mathbf{x} \in S \quad (2.3)$$

where the integration sign with a superimposed = indicates an integration in the sense of the finite part. This system of equations has a solution except when  $k$  coincides with

one of the eigenfrequencies of the homogeneous problem associated with our boundary value problem.

In engineering applications one usually discretises these equations with the help of certain shape functions and collocation, and then solves the resulting algebraic equations numerically. It has been shown, however, that the use of  $C^1$  elements for  $\varphi$  is necessary in order to obtain a good numerical solution of (2.3) with collocation [2]. This requirement is a big burden in 3D problems because it is difficult to generate  $C^1$  shape functions on a surface, although it is not in 2D since one may for example use spline functions. We therefore choose to use a variational approach in the discretisation of (2.3), even in 2D, because this approach allows the use of  $C^0$  elements and because we are interested in formulations applicable to 3D problems as well. Another benefit of the variational approach in numerical analyses is that it reduces the hypersingular integral in (2.3) to an ordinary one. This reduction of the singularity is called “regularisation” in the community of BIEM users. This technique, however, should not be confused with Tikhonov’s regularisation. We shall return to the detail of this approach in the next section.

We now proceed to the inverse problem mentioned in the introduction. This problem is now formulated as follows: Given  $M$  pairs  $(\overset{\circ}{u}^I, \partial \overset{\circ}{u}^I / \partial n)$ , ( $I = 1 \sim M$ ) on  $\partial D$ , find a crack  $S$  in a way that there exists a function  $u^I(\mathbf{x})$  ( $\mathbf{x} \in D \setminus \bar{S}$ ,  $I = 1 \sim M$ ) which satisfies (1.1)  $\sim$  (1.3) and

$$u^I = \overset{\circ}{u}^I, \quad \frac{\partial u^I}{\partial n} = \frac{\partial \overset{\circ}{u}^I}{\partial n} \quad \text{on } \partial D. \quad (I = 1 \sim M) \quad (2.4), (2.5)$$

As regards the uniqueness of the solution when there exists at least one solution  $S$ , we use arguments similar to the one in [5] to show that there cannot be more than one such  $S$  for a sufficiently large but finite  $M$ . In the special case of  $k = 0$ , Friedman & Vogelius[6] showed that 2 experiments ( $M = 2$ ) are sufficient for the uniqueness. It appears that their result has not been extended to the cases where  $k$  is non-zero. However, in the particular case of straight cracks, we can show in an almost trivial

manner that 2 experiments imply the uniqueness in the following sense: Let  $k$  be none of the Dirichlet (or Neumann) eigenvalues for  $D$ , and let  $U^I$  be the solution of

$$(\Delta + k^2)U^I = 0 \quad \text{in } D \quad \text{and} \quad U^I = \overset{\circ}{u}^I \quad \left( \text{or } \frac{\partial U^I}{\partial n} = \frac{\partial \overset{\circ}{u}^I}{\partial n} \right) \quad \text{on } \partial D. \quad (2.6)$$

Then there cannot be more than one straight crack with which (1.1)  $\sim$  (1.3), (2.4) and (2.5) are satisfied if

$$\det(\nabla U^1, \nabla U^2) \neq 0 \quad (2.7)$$

everywhere in  $D$ . Indeed, suppose that there are two cracks  $S_\alpha$  ( $\alpha = 1, 2$ ) which satisfy all the requirements. The corresponding solutions to the direct problems are denoted by  $u_\alpha^I$ . Then the difference  $u_1^I - u_2^I$  ( $I = 1, 2$ ) is identically zero in  $D \setminus (\overline{S_1 \cup S_2})$  by analytical continuation. The representation of the solution given in (2.1), however, shows that  $\varphi_\alpha^I$ , defined in an obvious manner, vanishes almost everywhere on  $S_\alpha$  ( $\alpha = 1, 2$ ), because

$$\varphi_1^I = u_1^{I+} - u_1^{I-} = u_2^{I+} - u_2^{I-} = 0 \quad \text{almost everywhere on } S_1,$$

etc. But this means  $u_\alpha^I = U^I$ , which is a contradiction because one cannot have (1.2) with  $u_\alpha^I = U^I$  ( $I = 1, 2$ ) at any point in  $D$  by virtue of the assumption in (2.7).

We remark that the restriction on  $k$  is eliminated if one defines  $U^I$  by

$$-U^I = g^I := \int_{\partial D} \frac{\partial G(\mathbf{x} - \mathbf{y})}{\partial n_y} \overset{\circ}{u}^I(\mathbf{y}) ds_y - \int_{\partial D} G(\mathbf{x} - \mathbf{y}) \frac{\partial \overset{\circ}{u}^I(\mathbf{y})}{\partial n} ds_y. \quad (2.8)$$

This choice, however, is not very convenient in practice.

In general our inverse problem may not have a solution. Guided by (2.2) and (2.3), however, we consider the following minimisation problem:

$$\text{Minimise } J(S) \quad \text{subject to } S \in D,$$

where the cost function  $J(S)$  is defined as follows: Give  $S$  arbitrarily. Solve (See (2.3) and (2.8).)

$$\frac{\partial g^I(\mathbf{x})}{\partial n} = \int_S \frac{\partial}{\partial n_x} \frac{\partial}{\partial n_y} G(\mathbf{x} - \mathbf{y}) \varphi^I(\mathbf{y}) ds_y, \quad \mathbf{x} \in S, \quad (2.9)$$

for the unknown  $\varphi^I$  on the given  $S$ . Notice that  $g^I$  is known since both  $\overset{\circ}{u}^I$  and  $\partial \overset{\circ}{u}^I / \partial n$  are. Define  $J(S)$  (See (2.2).) by

$$J(S) = \frac{1}{2} \sum_I \int_{\partial D} \left| \frac{\overset{\circ}{u}^I(\mathbf{x})}{2} - \int_{\partial D} G(\mathbf{x} - \mathbf{y}) \frac{\partial \overset{\circ}{u}^I(\mathbf{y})}{\partial n} ds_y \right. \\ \left. + \int_{\partial D} \frac{\partial G(\mathbf{x} - \mathbf{y})}{\partial n_y} \overset{\circ}{u}^I(\mathbf{y}) ds_y - \int_S \frac{\partial G(\mathbf{x} - \mathbf{y})}{\partial n_y} \varphi^I(\mathbf{y}) ds_y \right|^2 ds.$$

The most plausible crack  $S$  is then obtained as the minimiser of  $J(S)$ . In the next section we present a numerical method for solving this minimisation problem.

### 3. Numerical methods

3.1. Solution of singular integral equations As stated earlier, we prefer variational approaches in solving hypersingular integral equations. A variational equation associated with (2.9) is written as [7]

$$\int_S \frac{\partial \psi}{\partial s} ds \int_S G \frac{\partial \varphi^I}{\partial s} ds - k^2 \int_S \psi n_i ds \int_S G n_i \varphi^I ds = - \int_S \psi g_{,j}^I n_j ds. \quad (3.1)$$

where  $\psi$  is a test function which vanishes on  $\partial S$  and  $,_i := \partial / \partial x_i$ . The solution  $\varphi^I$  to (3.1) and (1.3) is unique. This equation could be solved numerically with Galerkin's method, but we prefer another approach which uses

$$\int_S G(\mathbf{x}_2 - \mathbf{y}) \frac{\partial \varphi^I(\mathbf{y})}{\partial s} ds_y - \int_S G(\mathbf{x}_1 - \mathbf{y}) \frac{\partial \varphi^I(\mathbf{y})}{\partial s} ds_y \\ + k^2 \int_{s(\mathbf{x}_1)}^{s(\mathbf{x}_2)} n_i(\mathbf{x}) \int_S G(\mathbf{x} - \mathbf{y}) n_i(\mathbf{y}) \varphi^I(\mathbf{y}) ds_y ds_x = \int_{s(\mathbf{x}_1)}^{s(\mathbf{x}_2)} g_{,i}^I(\mathbf{x}) n_i(\mathbf{x}) ds_x, \quad (3.2)$$

where  $\mathbf{x}_1$  and  $\mathbf{x}_2$  are points on  $S$ . Equation (3.2) is obtained by taking  $\psi$  to be piecewise constant on  $S$  in (3.1). In the numerical analysis based on (3.2) one introduces a certain discretisation to  $\varphi^I$  and takes as many pairs  $(\mathbf{x}_1, \mathbf{x}_2)$  as needed to determine unknowns in the discretised  $\varphi^I$ . Our experience shows that this approach is faster than Galerkin's method in 2D. In 3D, however, we use Galerkin which is more reliable than the 3D counterpart of (3.2). See [2] for details.

**3.2. Minimisation** In practice one may introduce simplifying assumptions on the shape of  $S$  and describe  $S$  by some shape parameters. For example, the assumption that  $S$  is a straight line enables us to identify  $S$  by 4 parameters, e.g. the coordinates of the tips. Since the cost function  $J(S)$  is now a function of these parameters, we can minimise it by using non-linear programming techniques such as Powell's variable metric method, which is our choice. This non-linear programming method, however, needs derivatives of  $J(S)$  with respect to the shape parameters, which are computed as

$$j(S) = \sum_I \operatorname{Re} \left\{ \int_S \left[ e_{ji} \dot{x}_j \frac{\partial \varphi^I}{\partial s} - n_i \dot{\varphi}^I \right] ds \int_{\partial D} G_{,i} \overline{F^I} ds + k^2 \int_S \varphi^I \dot{x}_i n_i \int_{\partial D} G \overline{F^I} ds \right\}, \quad (3.3)$$

where the superposed dot signifies one of such derivatives,  $e_{ij}$  indicates the permutation symbol,  $\overline{\phantom{x}}$  stands for the complex conjugate and

$$F^I(\mathbf{y}) = \frac{\dot{u}^I(\mathbf{x})}{2} - \int_{\partial D} G(\mathbf{x} - \mathbf{y}) \frac{\partial \dot{u}^I}{\partial n}(\mathbf{y}) ds_y + \int_{\partial D} \frac{\partial G(\mathbf{x} - \mathbf{y})}{\partial n_y} \dot{u}^I(\mathbf{y}) ds_y - \int_S \frac{\partial G(\mathbf{x} - \mathbf{y})}{\partial n_y} \varphi^I(\mathbf{y}) ds_y.$$

Notice that all the quantities included in (3.3) except for  $\dot{\varphi}^I$  are known from the boundary data ( $\dot{u}^I$ ,  $\partial \dot{u}^I / \partial n$ ) and the solution to (2.9). Also, the following variational equation for  $\dot{\varphi}^I$  is obtained as one takes the dot derivative of both sides of (2.9):

$$\begin{aligned} & \int_S \frac{\partial \psi}{\partial s} ds \int_S G \frac{\partial \dot{\varphi}^I}{\partial s} ds - k^2 \int_S \psi \frac{\partial x_i}{\partial s} ds \int_S G \frac{\partial y_i}{\partial s} \dot{\varphi}^I ds \\ & + \int_S \left\{ \frac{\partial \psi}{\partial s} g_{,i}^I e_{ij} - k^2 \psi g^I n_j \right\} \dot{x}_j ds \\ & + \int_S \frac{\partial \psi}{\partial s} ds \int_S G_{,j} (\dot{x}_j - \dot{y}_j) \frac{\partial \varphi^I}{\partial s} ds - k^2 \int_S \psi \frac{\partial x_i}{\partial s} ds \int_S G_{,j} (\dot{x}_j - \dot{y}_j) \varphi^I \frac{\partial y_i}{\partial s} ds \\ & - k^2 \left\{ \int_S \psi \frac{\partial \dot{x}_i}{\partial s} ds \int_S G \varphi^I \frac{\partial y_i}{\partial s} ds + \int_S \psi \frac{\partial x_i}{\partial s} ds \int_S G \varphi^I \frac{\partial \dot{y}_i}{\partial s} ds \right\} = 0. \end{aligned} \quad (3.4)$$

This equation can be solved numerically for  $\dot{\varphi}^I$  in a manner similar to the method of solving (3.1). In the special case of a straight crack (3.4) simplifies to

$$\int_S \frac{\partial \psi}{\partial s} ds \int_S G \frac{\partial \dot{\varphi}^I}{\partial s} ds - k^2 \int_S \psi ds \int_S G \dot{\varphi}^I ds$$

$$= - \int_S \left\{ \frac{\partial \psi}{\partial s} g_{,i}^I e_{ij} - k^2 \psi g^I n_j \right\} \dot{x}_j ds + k^2 \left( \frac{\partial \dot{x}_i}{\partial s} t_i \right) \int_S \psi ds \int_S G \varphi^I ds \quad (3.5)$$

In deriving (3.5) we have used integration by parts and the fact that  $\dot{x}_i$  is linear in the arc parameter  $s$ .

#### 4. Numerical examples

As a 2D numerical example we consider a circular domain  $D$  having a radius of  $r$ . The true crack is a linear one shown in Figure 1. We prescribe on  $\partial D$  2 Dirichlet data given by  $\dot{u}^I = e^{ikx_I}$  ( $I = 1, 2$ ), where the wave number is set equal to  $kr = 1$ . The corresponding Neumann data are obtained numerically rather than experimentally. 20% of error is given to  $\partial \dot{u}^I / \partial n - \partial U^I / \partial n$  on  $\partial D$ , where  $U^I$  is the solution to the Dirichlet problem introduced in (2.6). We modelled  $\partial D$  by 24 piecewise linear boundary elements and  $S$  by 9 node spline elements. The hypersingular integral equation in (2.9) is solved with (3.2). Figure 1(a) shows the crack configuration after every iteration step in an analysis which starts from the initial guess indicated in the same figure. This analysis converged to the crack location shown in Figure 1(b).

Obviously the same methodology applies to 3D problems as well; the numerical results of which have so far been obtained only in the Laplace case ( $k = 0$ ). The domain  $D$  and the crack  $S$  are assumed to be cubic and circular, respectively, as shown in Figure 2. The Dirichlet data given on the boundary are  $\dot{u}^I = x_I$  ( $I = 1 \sim 3$ ), and the corresponding Neumann data are computed via BIEM. No error in the data is considered. Galerkin's method is used to solve the 3D version of the hypersingular integral equation in (2.9). The exterior boundary is divided into 216 piecewise constant rectangular elements and the crack  $S$  is discretised with piecewise linear triangular elements having 21 DOF in total. An analysis starting from the initial guess shown in Figure 2(a) converged to the true crack location as indicated in Figure 2(b). Figure 2(b) also includes intermediate crack configurations after every (approximately) 5 iteration steps. The CPU time for this analysis was 12.4 sec. on Fujitsu VP400E (vector processor).

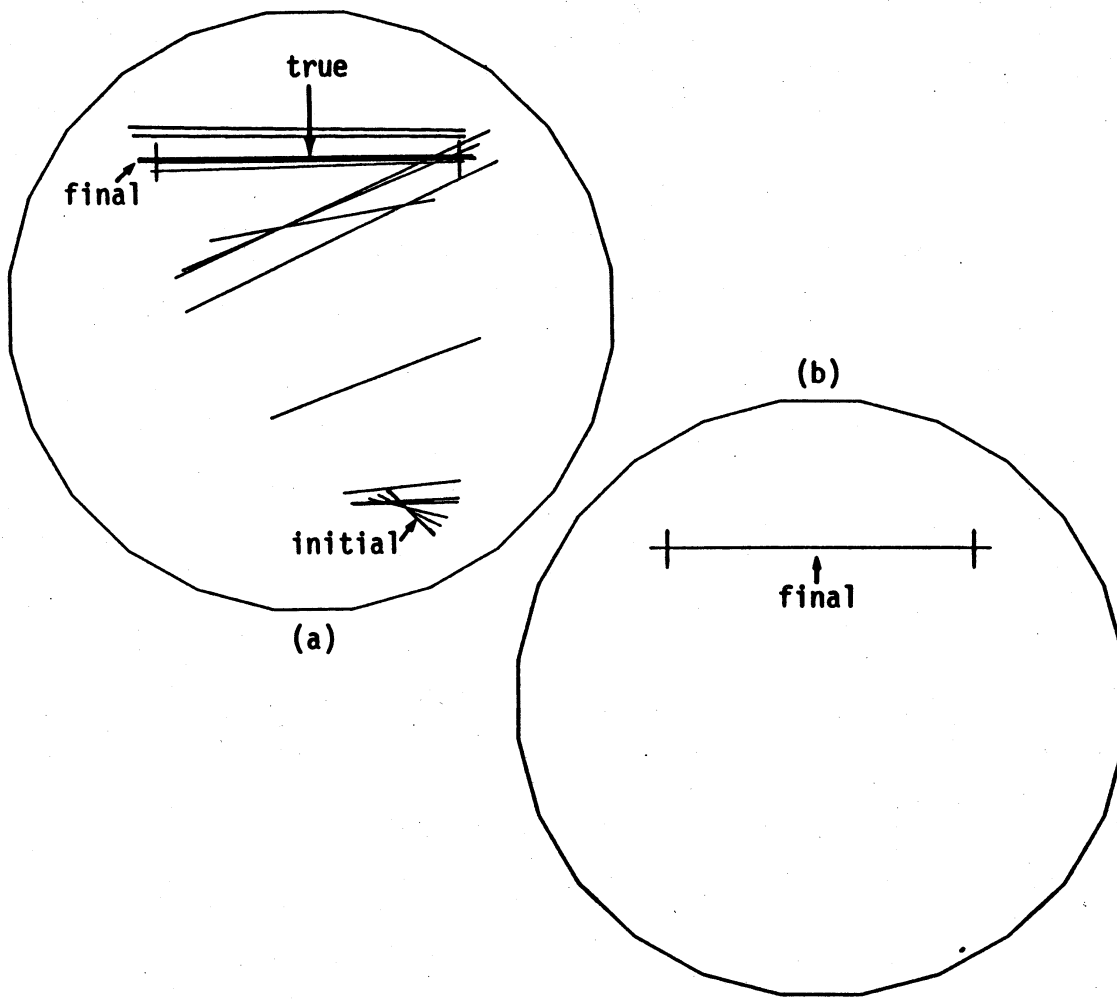


Figure 1: 2D crack detection analysis. (a) mode of convergence. (b) final result.

## 5. Concluding remark

In principle the method developed in this paper is applicable to 3D problems with non-zero wave numbers as well. Also a similar approach is possible in an analysis in the time domain. Investigations along these lines are now under way.

## References

- [1] Kubo, S. (1988) "Inverse problems related to the mechanics and fracture of solids and structures", *JSME Int. J.*, **31**, 157-66.

- [2] Nishimura, N. & Kobayashi, S. (1991) "A boundary integral equation method for an inverse problem related to crack detection", to appear in *Int. J. Num. Meth. Eng.*
- [3] Colton, D. & Monk, P. (1987) "The numerical solution of the three-dimensional inverse scattering problem for time harmonic acoustic waves", *SIAM J. Sci. & Stat. Comput.*, **8**, 278–91.
- [4] Kress, R. (1989) *Linear Integral Equations*, Springer (Berlin).
- [5] Colton, D. & Sleeman, B.D. (1983) "Uniqueness theorems for the inverse problem of acoustic scattering", *IMA J. Appl. Math.*, **31**, 253–9.
- [6] Friedman, A. & Vogelius, M. (1989) "Determining cracks by boundary measurements", IMA preprint series #476.
- [7] Hamdi M.A. (1981) "Une formulation variationnelle par équations intégrales pour la résolution de l'équation de Helmholtz avec des conditions au limites mixtes", *C. R. Acad. Sci. Paris (série II)*, **292**, 17–21.

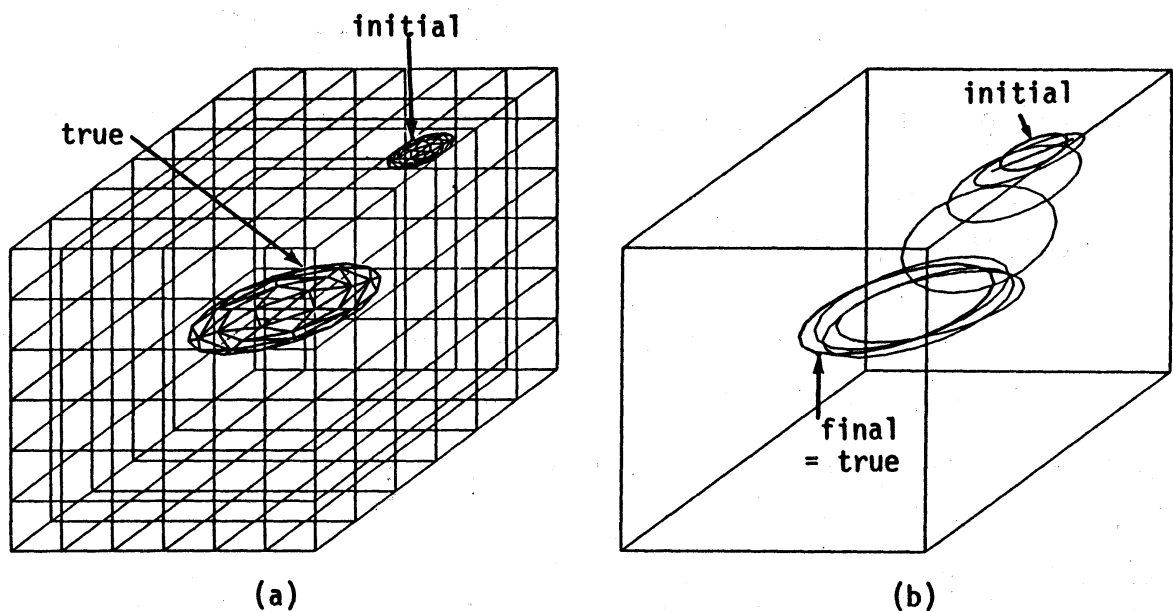


Figure 2: 3D crack detection analysis (Laplace). (a) mesh, initial guess and true crack. (b) mode of convergence.